

Article

Drivers of *Hymenoscyphus fraxineus* Infections in the Inner-Alpine Valleys of Northwestern Italy

Guglielmo Lione ^{1,2}, Silvia Ongaro ¹, Simona Prencipe ¹, Marianna Girauda ¹ and Paolo Gonthier ^{1,2,*}

¹ Department of Agricultural, Forest and Food Sciences (DISAFA), University of Torino, Largo P. Braccini 2, I-10095 Grugliasco, Italy; guglielmo.lione@unito.it (G.L.); silvia.ongaro@unito.it (S.O.); simona.prencipe@unito.it (S.P.); marianna.girauda@unito.it (M.G.)

² Interdepartmental Centre for Innovation in the Agro-Environmental Sector (AGROINNOVA), University of Torino, Largo P. Braccini 2, I-10095 Grugliasco, Italy

* Correspondence: paolo.gonthier@unito.it

Abstract: *Fraxinus excelsior* L. (ash) is a key forest tree species challenged by *Hymenoscyphus fraxineus* (T. Kowalski) Baral, Queloz, Hosoya, the causal agent of ash dieback. The goals of this study were (I) to assess the presence, spatial distribution, and incidence of *H. fraxineus* in the inner-alpine valleys of northwestern Italy, along with the severity of ash dieback; (II) to model the probability of infection by *H. fraxineus* based on environmental variables; (III) to reconstruct the direction of provenance of the front of invasion of the pathogen; and (IV) to test whether *H. fraxineus* has replaced the native relative *Hymenoscyphus albidus* (Gillet) W. Phillips, a saprobe of ash litter. By combining phytosanitary monitoring and samplings in 20 forest stands, laboratory analyses, and statistical modelling, this study showed that *H. fraxineus* was present in 65% of stands with an average incidence of 27%, reaching peaks of 80%. Rainfalls were the most relevant drivers of the probability of infection by *H. fraxineus*, rising up to 80% with the increased precipitation in April and July. Other drivers included elevation, maximal temperatures, latitude, and longitude. The front of invasion likely moved from Italy and/or Switzerland, rather than from France, while the replacement of *H. albidus* is uncertain.

Keywords: alps; ash dieback; *Chalara fraxinea*; climate; diagnostics; epidemiology; *Fraxinus excelsior*; infection; invasion biology; modelling; phytosanitary monitoring



Citation: Lione, G.; Ongaro, S.; Prencipe, S.; Girauda, M.; Gonthier, P. Drivers of *Hymenoscyphus fraxineus* Infections in the Inner-Alpine Valleys of Northwestern Italy. *Forests* **2024**, *15*, 732. <https://doi.org/10.3390/f15040732>

Academic Editor: Simon Francis Shamoun

Received: 7 March 2024

Revised: 18 April 2024

Accepted: 19 April 2024

Published: 22 April 2024



Copyright: © 2024 by the authors. Licensee MDPI, Basel, Switzerland. This article is an open access article distributed under the terms and conditions of the Creative Commons Attribution (CC BY) license (<https://creativecommons.org/licenses/by/4.0/>).

1. Introduction

Alpine forests are challenged by a variety of biotic, abiotic, and anthropogenic threats, reducing their ability to provide key ecosystem services. Such threats encompass the onset of epidemics caused by plant pathogens, some of which determine substantial mortality and economic losses [1]; attacks by insect pests [2]; natural or anthropogenic disturbances [3,4]; and climate change [5].

In northwestern Italy, especially in the inner Alps of the Aosta Valley region hosting the highest mountains in Europe, the European or common ash (*Fraxinus excelsior* L., hereafter referred to as ash) is a companion species growing up to 1400 m a.s.l. in mixed forest stands in association with several broadleaved or conifer species of the genera *Acer*, *Alnus*, *Carpinus*, *Castanea*, *Corylus*, *Larix*, *Pinus*, *Prunus*, *Tilia*, *Ulmus*, and others [6]. Ash trees are generally not abundant, although they can be prevalent in forest patches of a limited surface area or when they colonize abandoned agricultural fields or grasslands in close proximity to forest stands [6,7]. Ash is scored as a key species for the functioning and conservation of forest ecosystems; hence, its long-term preservation is deemed a priority [8].

A major challenge threatening the conservation of ash in Europe is the “ash dieback” caused by the fungal pathogen *Hymenoscyphus fraxineus* (T. Kowalski) Baral, Queloz, Hosoya, comb. nov. (an ascomycete formerly described as *Chalara fraxinea* or *H. pseudoalbidus*) [9,10]. *H. fraxineus* was likely introduced to Europe by means of infected plant material from Asia. Ash dieback was first reported in Poland in association with the

extensive mortality of ash trees during the early 1990s [9,11]. Since then, *H. fraxineus* has rapidly spread across most of the geographic distribution area of ash in Europe [12] posing a serious threat to ash and other organisms closely dependent upon the presence of ash [13]. The disease symptoms include the leaves withering and wilting, followed by the onset of necrotic spots on the leaf laminae leading to their progressive deformation. Necrosis may also affect the petioles and rachises of the leaves, whose premature fall subsequently occurs. *H. fraxineus* may also colonize shoots, twigs, and branches by affecting the cambium, thereby causing sunken areas and cankers visible as longitudinal lesions of the bark. The combination of the fall of the leaves and the desiccation of the branches leads to a progressive crown thinning and loss, resulting in the overall decline of the tree. The crown loss induced by *H. fraxineus* on ash follows a typical and recognizable pattern, starting from the upper and external sectors and progressing towards the lower and inner portions. This phenomenon is commonly defined as “dieback”, ultimately leading to the death of the tree. Additional symptoms may include a color alteration of the bark in the basal portion of the main stem, which can display the occurrence of lesions.

The impact of ash dieback in Europe has been detrimental, leading to substantial direct and indirect economic losses mainly related to the reduced or zeroed profit from nurseries and productive forests, the costs of the silvicultural or other management operations needed to fell and replace the infected and dead trees, and the depletion of the ecosystem services provided by ash [14,15]. The highest economic losses reported by Hill et al. (2019) [14] were generated by the effects of ash dieback on the ecosystem services. The impact of the disease has achieved relevant magnitude levels as a result of the high incidence of the pathogen, of the severity of the symptoms, and of the substantial mortality affecting ash trees of all ages in forest, plantations, and nurseries [14,16,17]. Indeed, a meta-analysis conducted on data gathered at the European scale reports the peaks of ash mortality reaching approximately 85% in plantations, 70% in forest, and 82% in natural regenerated saplings [17].

The impact of *H. fraxineus* may be relevant not only for ash as a forest tree species but also for the other species directly associated with ash [8], potentially leading to biodiversity losses and, in the worst case, to the local extinction of some taxa (i.e., leading to an “extinction cascade”) [13]. Some invasive forest pathogens are capable of colonizing newfound hosts or habitats while replacing native species, even congeners, as documented for the invasive vs. native pathogens: *Heterobasidion irregulare* Garbel. & Orosina and *H. annosum* (Fr.) Bref. [18]; *Phytophthora ramorum* Werres, De Cock & Man in ‘t Veld and *P. nemorosa* E.M. Hansen & Reeser [19]; and *Ophiostoma novo-ulmi* Brasier and *O. ulmi* (Buisman) Nannf. [20]. In the case of *H. fraxineus*, a similar phenomenon has been reported, with the invasive pathogen replacing the congeneric yet saprobic fungus *Hymenoscyphus albidus* (Gillet) W. Phillips, a decomposer of ash litter [21] and harmless ash endophyte [22].

The biological cycle of *H. fraxineus* has been thoroughly investigated [10,16,23,24]. In brief, at the end of summer, the pathogen produces typical pedunculate whitish apothecia in the litter on the rachises and petioles of the ash that fell the previous year. Infectious airborne ascospores are released from the apothecia and infect the green leaves of ash trees. Ascospores represent the main source of inoculum allowing the short and long distance dispersal of *H. fraxineus*. While it was estimated that most of the ascospores spread up to 2.6 km from their source [25], air turbulence may allow their dissemination at distances of 50–100 km [26,27]. Consequently, the front of the disease can progress rapidly, as reported in previous studies, which identified a spread rate of 30 km/year in Norway [16], 40–50 km/year in central Italy [28], and 50 km/year in France [25,27]. In northern Italy, based on the first report of the pathogen in 2009 in the east (the Friuli region) [29] and on the following detection of the pathogen in the west (the Piedmont region) in 2016 [30], the spread rate was estimated as high as 70 km/year.

The success of biological invasions in forest ecosystems may depend upon several interacting factors, including the site, the host, and the environmental and climatic suitability that fosters the establishment and spread of the pathogen and the expression of the disease symptoms [31]. The applications of modelling and numerical ecology may shed light on

the most relevant ecological drivers boosting or hampering biological invasions [32]. In the case of ash dieback, several studies so far have investigated which ecological factors may be favorable, or not, to *H. fraxineus* (a comprehensive review is presented in [33]). For instance, environmental and silvicultural variables were tested to unravel the putative predisposing condition boosting the onset and impact of the disease in the Czech Republic [34], and a similar approach was used to relate the site, stand, and landscape features to the disease in France [35,36]. A large-scale modelling was aimed at elucidating the role of some environmental and climatic variables on the risk of the natural spread of *H. fraxineus* at the European level, also including some bordering areas of Africa and Asia [37]. Other studies related the tree host's age, sex, provenance, and dendrometric features to the severity of the disease, while some research has been conducted to assess the role of forest management practices on ash dieback [38–40].

Although relevant information about the European distribution of *H. fraxineus* and the factors potentially associated with its successful establishment and spread are reported in the literature, there are still relevant geographic sectors for which no information is currently available. This is the case of the inner Alps of the Aosta Valley representing one of the most relevant Alpine sectors, of which 27% is covered by forests [6]. To date, it is still unknown whether ash dieback caused by *H. fraxineus* is present in that area and which factors might have played a role in the onset of the disease, if any. In addition, any models quantitatively assessing the probability of infection by *H. fraxineus* based on environmental and site conditions are scanty. Hence, the goals of this work were (I) to assess the presence, spatial distribution, and incidence of *H. fraxineus* in the inner-alpine valleys of northwestern Italy, along with the severity of ash dieback; (II) to model the probability of infection by *H. fraxineus* based on topographic, geomorphologic, dendrometric, and climatic variables; (III) to reconstruct the direction of provenance of the front of invasion of the pathogen; and (IV) to test whether a replacement of *H. albidus* with *H. fraxineus* has occurred.

2. Materials and Methods

2.1. Study Sites and Ash Tree Selection

Based on data about the spatial distribution of ash in the Aosta Valley [6] and on surveys conducted by the Forestry Corps of the Region (Corpo Forestale della Valle d'Aosta-Dipartimento Risorse naturali e Corpo forestale), a total of 20 representative study sites were selected. All sites hosted several hectares of uneven aged forest stands characterized by a mixed tree species composition including broadleaves (*Acer* spp., *Alnus* spp., *Betula pendula*, *Castanea sativa*, *Corylus avellana*, *Populus tremula*, *Salix* spp., *Prunus avium*, *Quercus pubescens*, *Robinia pseudoacacia*, *Sorbus aucuparia*, and *Tilia* spp.) and conifers (*Abies alba*, *Larix decidua*, *Picea abies*, and *Pinus sylvestris*), where ash was present sporadically, with an abundance generally between 5% and 35%, although reaching 85% in one site. The ash abundance was scored based on the inventory data provided by the Forestry Corps. For each study site, the longitude (x) and latitude (y) (UTM WGS1984 reference system, in m) were recorded with a GPS device (MobileMapper[®], Magellan, LA, USA—precision ± 1 m) in the WGS84/UTM projection system. Each study site was assigned to a specific geographic sector (*sect*) of the Aosta Valley (high, medium, and low sectors) based on the classification reported in [41]. The site elevation (el , in m a.s.l.) was obtained from the Digital Terrain Model (DTM) [42], queried through the Geographic Information System (GIS) software QGIS version 3.4.7 [43], based on the pixel value corresponding to the associated x and y coordinates. The maps to assess the aspect (as , as azimuth, in $^{\circ}$) and slope (sl , in $\%$) of the study sites were derived from the DTM, as described in Lione et al. (2017) [32].

Within each study site, a number of ash trees was selected for the assessment of dieback symptoms and for the sampling of plant tissues, based on the following method. The first tree was randomly chosen, then up to 4–8 of its surrounding nearest neighbors growing within a distance radius of 15 m were selected. The dendrometric variables measured for each of the above mentioned ash trees were the diameter at breast height (dbh ,

in cm), obtained by using a tree caliper; and the tree height (h , in m), assessed through a hypsometer (PM-5/1520 Series, Suunto, Vantaa, Finland). The summary of the geographic (x , y , and $sect$), geomorphologic (el , sl , and as), and dendrometric (dbh and h) variables of each study site is reported along with the main tree species composition and abundance in Table 1.

Table 1. Study sites monitored for ash dieback. For each site, the code, location, municipality, geographic, and geomorphologic details are reported along with the corresponding dendrometric characteristics and the abundance of the ash trees. The acronyms are specified in the footnotes.

Site Code	Location (Municipality)	x ¹	y ²	el ³	$sect$ ⁴	sl ⁵	as ⁶	dbh ⁷	h ⁸	ab ⁹
A	Entreves (Courmayeur)	341,316	5,075,640	1307	H	16.8	211	15.9 (6.2)	10.8 (4.0)	20
B	Chabodey (La Salle)	349,002	5,066,317	1192	H	43.0	52	6.0 (2.1)	9.1 (2.5)	15
C	Lenteny (La Salle)	350,448	5,065,962	851	H	0.5	45	12.8 (11.7)	12.6 (8.7)	10
D	Valsavarenche (Valsavarenche)	359,759	5,055,843	1239	H	36.4	261	8.7 (2.5)	8.8 (2.6)	15
E	Buillet (Introd)	358,546	5,060,513	979	H	97.3	334	12.0 (2.2)	12.2 (2.8)	10
F	Courmayeur (Courmayeur)	341,788	5,074,415	1246	H	39.1	95	6.4 (2.1)	7.7 (1.3)	10
G	Verrand (Pré-Saint-Didier)	342,429	5,071,661	1189	H	40.0	211	10.9 (4.1)	12.1 (3.6)	35
H	Elevaz (Pré-Saint-Didier)	341,679	5,067,384	1273	H	65.8	141	10.7 (8.5)	9.7 (6.3)	25
I	Fenêtre (La Salle)	351,287	5,066,944	1117	H	73.6	149	12.9 (6.2)	11.7 (2.7)	35
L	Derby (La Salle)	351,324	5,065,019	847	H	35.3	52	13.2 (7.6)	10.9 (4.4)	10
M	Croix Blanche (Villeneuve)	359,789	5,061,355	886	H	37.0	304	6.9 (1.4)	8.2 (1.5)	5
N	Chessin (Antey-Saint-André)	390,441	5,070,429	785	L	13.0	129	14.8 (6.1)	11.6 (3.3)	15
O	Arbaz (Challand-Saint-Anselme)	401,107	5,063,836	1380	L	72.5	118	9.1 (5.8)	7.0 (1.9)	15
P	Bois de Cretes (Challand-Saint-Anselme)	402,035	5,061,547	900	L	18.4	334	17.5 (5.2)	19.4 (4.0)	85
Q	Grand Brissogne (Brissogne)	375,765	5,063,852	1122	M	44.7	70	11.2 (7.2)	10.0 (3.9)	10
R	Pied de Ville (Valpelline)	373,024	5,076,999	1089	M	53.7	348	11.2 (5.4)	6.1 (1.9)	5
S	Étroubles (Étroubles)	362,853	5,075,438	1280	M	27.1	183	10.3 (7.2)	6.4 (2.1)	15
T	Rean (Saint-Marcel)	380,784	5,065,119	836	M	3.3	302	20.4 (12.5)	17.4 (5.0)	10
U	La Fabbrica (Valpelline)	369,490	5,075,094	895	M	46.2	307	6.8 (2.2)	9.0 (2.0)	10
V	Pont (Saint-Rémy-en-Bosses)	358,069	5,075,298	1483	M	20.7	319	22.7 (12.4)	17.0 (4.9)	20

¹ longitude (m, UTM WGS84 zone 32 N); ² latitude (m, UTM WGS84 zone 32 N); ³ elevation (m a.s.l.); ⁴ sector of the Aosta Valley (H: high, M: medium, L: low); ⁵ slope (°); ⁶ aspect (azimuth, °); ⁷ average diameter at breast height (cm) of the ash trees with corresponding standard deviation in brackets; ⁸ average tree height (m) of the ash with corresponding standard deviation; and ⁹ ash abundance (%).

2.2. Assessment of Ash Dieback Symptoms and Plant Tissue Samplings

Based on the description of the symptoms of ash dieback [8,12,44], three variables were assessed to score the health status of the selected trees: the crown transparency ($crtr$, in %), the percentage of leaves displaying necrotic areas on the lamina (pnl , in %), and the number of lesions observed at the stem base (nl , as count). The crown transparency was appraised by using the method reported in [45,46] and as described in [47]. In brief, the crown transparency was visually assessed scoring the loss of leaves (%) in relation to an ideal status where defoliation is absent, with the operator located at a distance from the stem base corresponding to the tree height or at the closest distance allowing a complete view of the crown. The percentage of the leaves showing symptoms of necrosis was assessed by calculating the ratio between the number of symptomatic leaves and the total number of leaves collected per tree. The number of leaves sampled per tree varied between six and thirty, depending on the accessibility of the branches present in the lower portion of the crown, which were excised by using a telescopic tree lopper extendable up to 5 m. Overall, approximately 200 branches were collected from 88.5% of the selected ash trees, while the

remaining 11.5% were not sampled. The number of lesions at the base stem was assessed by carefully inspecting the base of the trees and excluding mechanical lesions caused by ungulates or other animals, wounds resulting from the failures of neighboring trees, etc.

The plant tissues were collected from the selected ash trees to conduct the diagnostic analyses targeting *H. fraxineus* and *H. albidus* (see Section 2.3). In detail, a total of 107 foliar and 92 wood samples were collected, with the first obtained from the branches excised for the assessment of the percentage of necrotic leaves and the latter in proximity of the basal stem lesions. In the absence of visible lesions, wood chips were randomly excised from the stem. For both symptomatic and asymptomatic ashes, the wood chips of an approximate dimension of 5 × 2 × 0.5 cm were carved with a chisel previously disinfected with a commercial solution of sodium hypochlorite (NaClO). In addition, the litter within a 1.5 m radius from the base of the selected ash trees was carefully inspected to identify and collect the rachises and petioles of *F. excelsior* harboring apothecia morphologically compatible with those formed by *H. fraxineus* or *H. albidus*, based on the description and plates reported in [48].

The samples collected were singly placed in plastic bags (for the foliar samples and wood chips) or 15 mL centrifuge tubes (for the rachises and petioles), immediately transported to the laboratory, and stored at +4 °C prior to further processing. Both the assessments of the ash dieback symptoms and the samplings were conducted between June and September in 2020 and 2021.

2.3. Laboratory Analyses

Laboratory analyses were conducted on the leaves and wood samples to detect the presence of *H. fraxineus*, *H. albidus*, or both, through species-specific quantitative Polymerase Chain Reaction (qPCR) assays, conducted as described below. The plant tissue fragments to analyze were excised with a sterile scalpel at the interface between the symptomatic and asymptomatic portions of the samples, when symptoms were present. For the samples showing no symptoms, the plant tissues to collect were randomly selected. DNA was extracted from 20 mg of plant tissues obtained after a 24 h lyophilization phase followed by a 30 min grinding step performed with a Tissue Lyser (Qiagen, Hilden, Germany) set at 30 Hz. The extraction was carried out using the DNeasy® Plant Mini Kit (Qiagen) following the manufacturer's instructions with minor modifications. Genomic DNA was amplified using the primers and probes for the specific detection of *H. fraxineus* (Cf-F, Cf-R, and Cf-S) [49] and *H. albidus* (Halb-F, Halb-R, and Halb-P) [50] (Table 2).

Table 2. Species specific primers and probes used for the qPCR analyses for the specific detection of *Hymenoscyphus fraxineus* and *H. albidus*.

Primer/Probe Name	Sequence (5'-3')	References
Cf-F	CCCTTGTGTATATTATATTGTTGCTTTAGC	[49]
Cf-R	GGGTCCTCTAGCAGGCACAGT	[49]
Cf-S	6FAM-TCTGGGCGTCCGCCTCGG-BHQ1	[49]
Halb-F	TATATTGTTGCTTTAGCAGGTCGC	[50]
Halb-R	ATCCTCTAGCAGGCACGGTC	[50]
Halb-P	HEX-CCGGGGCGTTGGCTCG-BHQ2	[50]

The amplifications were carried out using the thermal cycler Real Time CFX Connect™ (BioRad, Hercules, CA, USA) with 96 well-plates (Biorad) sealed with Microseal® B seal adhesive film (Biorad). The reactions were carried out using an SsoAdvanced Universal Probes Supermix 2× (Bio-Rad, USA). The amplification conditions were 95 °C for 10 min, followed by 40 cycles of 95 °C for 15 s and 59 °C for 1 min for the *H. fraxineus*. After each run, one cycle of the melting curve step was conducted by ramping the temperature from 60 °C to 90 °C. The reactions were carried out in a final volume of 10 µL, with 3 µL of DNA,

0.25 μL of each primer (10 μM), 0.50 μL of the probe (5 μM), and 5 μL of the SsoAdvanced Universal Probes Supermix 2 \times (Bio-Rad).

The specific amplification conditions for the *H. albidus* were 95 $^{\circ}\text{C}$ for 10 min, followed by 35 cycles of 95 $^{\circ}\text{C}$ for 15 s and 64 $^{\circ}\text{C}$ for 55 s. The reactions were carried out in a final volume of 10 μL , with 3 μL of DNA, 0.30 μL of each primer (10 μM), 0.15 μL of the probe (10 μM), and 5 μL of the SsoAdvanced Universal Probes Supermix 2 \times (Bio-Rad). Each 96-well plate was loaded in triplicate with a negative control (RNase free water), standard DNA, and a positive control (the *H. fraxineus* DNA strain KNE31P or the *H. albidus* DNA strain H8945). In order to validate the results of the positive amplifications obtained with the qPCR assay, 13 representative amplicons were sequenced in both directions by BMR Genomics, with primers used for the amplification. By using the BLASTN tool of the NCBI, the obtained sequences were compared with those deposited in GenBank.

2.4. Climatic Characterization of the Study Sites

For all the study sites, the spatial coordinates x , y , and el were stored in a dataset and combined with the corresponding coordinates of the available weather stations included within the Aosta Valley official meteorological network (i.e., the Centro Funzionale e Pianificazione Regione Autonoma Valle d'Aosta). Each study site was characterized by a set of 80 climatic variables, obtained as described below.

Only the official meteorological weather stations providing at least the daily maximum, minimum, and average temperatures, precipitation, and wind speeds were retained. The three-dimensional Euclidean distance $d = \sqrt{\Delta x^2 + \Delta y^2 + \Delta el^2}$ was calculated [51], with Δx , Δy , and Δel representing the differences of longitude, latitude, and elevation separating each study site from the retained weather stations. Up to four of the nearest neighboring weather stations with $d < 10.5$ km were assigned to each sampling site, and the time series of the 10 years preceding the date of the samplings were filtered. From these time series, the monthly average values of the maximum ($tmax_i$), minimum ($tmin_i$), and mean ($tmean_i$) temperatures (in $^{\circ}\text{C}$); cumulated rainfall precipitation (p_i) (in mm); and windspeed (ws_i) (in m/s) were calculated for months $i = \{1, 2, 3, 4, 5, 6, 7, 8, 9, 10, 11, 12\}$, representing the months from January ($i = 1$) to December ($i = 12$). The same values were calculated at a seasonal level with $i = \{fa, sp, su, wi\}$ for fall, spring, summer, and winter, respectively, as reported in [52]. The study sites were combined with the corresponding climatic variables at the monthly and seasonal levels by calculating the spatial weighted averages for all possible values of the index

i [53,54] as follows: $Tmax_i = \frac{\sum_{j=1}^{j=n} w_j tmax_{i,j}}{\sum_{j=1}^{j=n} w_j}$; $Tmin_i = \frac{\sum_{j=1}^{j=n} w_j tmin_{i,j}}{\sum_{j=1}^{j=n} w_j}$; $Tmean_i = \frac{\sum_{j=1}^{j=n} w_j tmean_{i,j}}{\sum_{j=1}^{j=n} w_j}$;

$P_i = \frac{\sum_{j=1}^{j=n} w_j P_{i,j}}{\sum_{j=1}^{j=n} w_j}$; $Ws_i = \frac{\sum_{j=1}^{j=n} w_j ws_{i,j}}{\sum_{j=1}^{j=n} w_j}$, with n representing the number of weather stations

assigned to each study site and w as the weight value set to $\frac{1}{d}$. The weather stations' information is reported in Table S1.

2.5. Statistical Analysis and Modelling

The status (I) of each ash tree was binarily scored as infected ($I = 1$) or uninfected ($I = 0$) by *H. fraxineus*, based on the outcomes of the molecular analyses conducted on the plant tissue samples (see Section 3). The average levels of the ash dieback symptoms (i.e., the crown transparency, percentage of necrotic leaves, and number of lesions observed at the stem base, which are $crtr$, pnl , and nl , respectively) were compared between the infected and uninfected ashes with the Wilcoxon rank sum test [54]. The incidence of the pathogen was assessed as the ratio between the infected trees and the total number of sampled trees (in %).

The putative predictors of the probability of infection by *H. fraxineus* $Pr_{(I=1)}$ [55] (i.e., the response variable) were divided into blocks as follows: the dendrometric variables (dbh , h), the topographical variables (x , y , $sect$); the geomorphological variables (el , sl); and the climatic variables. For the latter, ten distinct blocks were built, accounting for the five variable types

($Tmax_i$, $Tmin_i$, $Tmean_i$, P_i , and Ws_i) and the two reference timeframes (monthly or seasonal) (i.e., five variable types \times two reference timeframes = ten blocks). Unbiased recursive binary partitioning tree models based on conditional inference [56–58], hereafter referred to as *ctree* models, were fitted to the response variable separately for each block of predictors by setting the algorithms as described in Lione et al. (2017, 2020) [32,47]. The p -value associated with each predictor was calculated based on the c -statistics [56–58], as reported in [52]. When the *ctree* identified the significant thresholds resulting from binary splits of the model, for each terminal node the value of the response variable was calculated with the equation $\frac{f(I=1)}{m}$, with f representing the indicator function with the Iverson notation [59] and m the number of the ash trees clustering within the node. The predictors whose p -values were significant ($p < 0.05$) were preselected for a further modelling step, conducted as described below.

The probability of infection by *H. fraxineus* was modelled as a function of the preselected variables, included in blocks (see above) or singularly, by fitting the binary logistic regression models [55] as generalized linear models (GLMs) [54]. The β coefficients of each logistic equation based on a number w of the preselected predictor variables v $Pr_{(I=1)} = \frac{e^{\beta_0 + \sum_{h=1}^{h=w} \beta_h v_h}}{1 + e^{\beta_0 + \sum_{h=1}^{h=w} \beta_h v_h}}$ were assessed with the Wald test [55]. In addition, the corresponding null model was fitted and singularly compared with the other logistic regressions by using the likelihood ratio test (LRT) [54,55] and the values of the Akaike Information Criterion (AIC) and of its associated weights (AICw) [60,61]. The classification performance of each logistic regression model was assessed by calculating the area under the relative operating characteristic curve (AUC) and its cross-validated 95% confidence interval, whose bounds were compared with the 0.5 threshold [62,63]. The overall assessment score of the models was based on the criteria reported in [47], thus accounting for the significance of the β coefficients, the LRT test, the bounds of the AUC 95% confidence interval, and ranking the performance of the models based on increasing the AICw and AUC values.

The association between the probability of infection by *H. fraxineus* and the aspect (*as*) of the study site was tested with a standalone analysis due to the circularity of the predictor [64], by using the method described in [32], based on the application of the Mardia–Watson–Wheeler test [65] and the Rao’s homogeneity test [66].

In order to analyze whether the impact of *H. fraxineus* resulted in a spatial gradient, the DirGrad algorithm [67] was applied to the incidence of the pathogen, assessed at the site level as the ratio between the infected trees and the total number of sampled trees (%), and to the variables *crtr*, *pnl*, and *nl*, associated with the symptoms of ash dieback assessed as described in Section 2.2. The gradient directions and the prevailing gradient direction were assessed with the criteria considering the sign and the magnitude of the index R , as reported in [67]. The direction from an octant O_1 ($R < 0$) to the opposite O_2 ($R > 0$) is expressed as $O_1 \rightarrow O_2$ ($\mp R$) [67]. The same algorithm was used to identify the spatial gradients of the monthly precipitation of April (P_4) and July (P_7), because these variables were significant predictors of the probability of infection by *H. fraxineus* in the best performing binary logistic regression model (see Section 3).

The statistical analysis and modelling were conducted with R version 4.0.0 (R Core Team, 2020), with the algorithm DirGrad [67] and the packages binGroup [68], bootstrap [69], circular [70] cvAUC [63], MuMIn [71], partykit [58], and strucchange [57]. The significance cut-off level was set at 0.05 [54]. The 95% confidence intervals ($CI_{95\%}$) were calculated with the method reported in Blaker [72] for the variable expressed as a percentage, while for the other variables the bootstrap Bias Corrected and accelerated (BCa) $CI_{95\%}$ were obtained based on DiCiccio and Efron (1996) [73] with the bootstrap algorithm set as described in Lione et al. (2020) [47].

3. Results

3.1. Incidence, Distribution, and Impact of *Hymenoscyphus fraxineus*

Overall, the phytosanitary survey targeting ash dieback caused by *H. fraxineus* in the inner-alpine valleys of northwestern Italy covered a region extending approximately 60 km in longitude and 20 km in latitude, corresponding to an area of 1200 km² with an elevation up to 1483 m a.s.l. The presence of *H. fraxineus* was detected through the qPCR species-specific assay in 13 out of the 20 study sites (65.0%, 42.2%–84.0% CI_{95%}), attaining an overall incidence (i.e., the percentage of infected ashes) of 27.0% (19.0%–36.4% CI_{95%}) and reaching a maximum value of 80% (Figure 1). Ash trees positive to the pathogen were detected in 20.3% (13.1%–29.1% CI_{95%}) of the cases from wood tissues, and in the remaining 6.7% (3.0%–13.2% CI_{95%}) of the cases from foliar tissues.

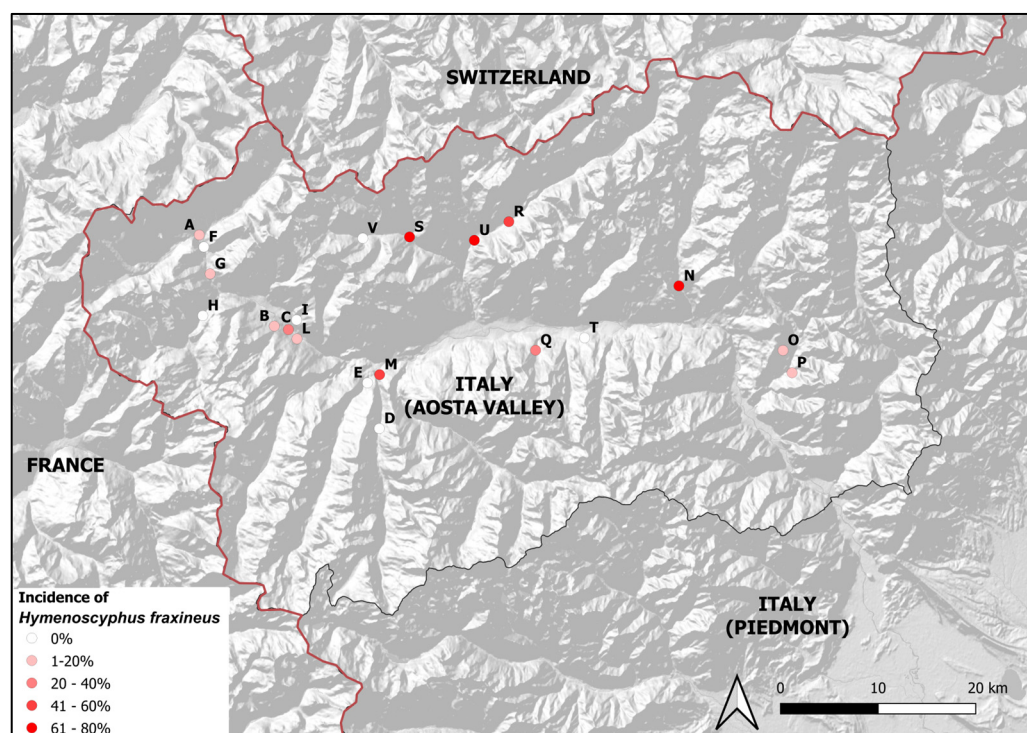


Figure 1. Map of the spatial distribution and incidence of *Hymenoscyphus fraxineus* in the inner-alpine valleys of northwestern Italy. For site acronyms, see Table 1.

The symptoms observed in the field included the crown transparency, leaves displaying necrotic areas on the lamina, and lesions at the stem base. The crown transparency (*crtr*) attained an overall average of 34.9% (30.3%–39.9% CI_{95%}), but, while the ash trees infected by *H. fraxineus* displayed crown losses of 47.0% (36.4%–57.8% CI_{95%}), those uninfected showed significantly lower values (30.4%, 25.9%–35.8% CI_{95%}, $p = 9.64 \cdot 10^{-3}$). Comparable patterns were observed for the other symptoms. Indeed, the percentage of leaves displaying necrotic areas on the lamina (*pnl*) achieved an overall mean of 31.1% (24.8%–38.4% CI_{95%}), with infected ash trees reaching an average of 45.8% (31.0%–61.2% CI_{95%}), significantly higher than the 26.3% (20.0%–34.2% CI_{95%}) resulting from uninfected trees ($p = 4.72 \cdot 10^{-2}$). Finally, the average number of stem lesions observed was 1.20 (0.95–1.48 CI_{95%}), but, while the ash trees infected by *H. fraxineus* displayed a mean of 1.67 (1.21–2.25 CI_{95%}), those uninfected attained a significantly lower value of 1.03 (0.75–1.37 CI_{95%}, $p = 6.57 \cdot 10^{-3}$).

3.2. Ecological and Environmental Variables Associated with the Probability of Infection by *Hymenoscyphus fraxineus*

The ecological and environmental variables significantly correlated ($p < 0.05$) to the probability of infection by *H. fraxineus* ($Pr_{(I=1)}$) that resulted from the *ctree* models fitting were as follows: the topographical variables latitude (x) and longitude (y); the geomorphological variable elevation (el); and the climatic variables related to the maximum temperature of December (T_{max12}), the monthly cumulated rainfall precipitation of April (P_4) and July (P_7), and the seasonal cumulated rainfall precipitation during the spring (P_{sp}). Instead, all the other tested variables did not result in significant c -statistics that produced tree graph splits ($p > 0.05$). In detail, the significant *ctree* models showed that at a high latitude and longitude (i.e., in the northeastern sector, $x > 358,069$ m, $y > 506,7384$ m) the probability of infection by *H. fraxineus* was maximal, attaining 75.0% (52.6%–89.6% $CI_{95\%}$), while it dropped significantly ($p < 0.05$) for those ash trees located in the southern ($y \leq 5,067,384$ m) and northwestern ($x \leq 358,069$ m, $y > 5,067,384$ m) sectors, whose $Pr_{(I=1)}$ was 17.2% (9.5%–28.6% $CI_{95\%}$) and 10.0% (1.8%–31.6% $CI_{95\%}$), respectively. Ash trees growing in the forest stands whose elevation was below 895 m a.s.l. resulted in a significantly ($p = 3.41 \cdot 10^{-2}$) higher probability of infection (46.7%, 29.5%–65.5% $CI_{95\%}$) than those located in the sites at higher altitudes (18.9%, 11.0%–29.4% $CI_{95\%}$). The sites whose maximum temperature in December was on average over 4.1 °C were characterized by ash trees whose probability of infection reached 44.9% (22.2%–59.3% $CI_{95\%}$), significantly surpassing the probability of 10.9% (4.9%–31.3% $CI_{95\%}$) displayed by the trees growing in cooler sites. The analysis conducted on precipitation showed that more abundant rainfalls during the months of April (P_4) and July (P_7) significantly boosted the likelihood of infection ($p < 0.05$), with probabilities $Pr_{(I=1)}$ at 80.0% (53.5%–94.3% $CI_{95\%}$) in the rainiest locations ($P_4 > 41.2$ mm and $P_7 > 62.3$ mm), decreasing to 26.7% (14.8%–41.1% $CI_{95\%}$) in the sites with high precipitation levels in April ($P_4 > 41.2$ mm) but low rainfalls in July ($P_7 \leq 62.3$ mm), and dropping to 9.1% (3.1%–21.0% $CI_{95\%}$) where the two months of April and July were drier ($P_4 \leq 41.2$ mm and $P_7 \leq 62.3$ mm). Consistently, spring rainfalls over 161 mm led to a probability $Pr_{(I=1)}$ of 51.4% (25.0%–67.5% $CI_{95\%}$), significantly higher ($p = 8.61 \cdot 10^{-3}$) than that achieved when precipitation in spring was under the above threshold (14.5%, 7.5%–34.9% $CI_{95\%}$). A detailed list of the statistics resulting from the *ctree* models is reported in Table S2.

The probability of infection by *H. fraxineus* modelled as a function of the variables preselected by the *ctrees* resulted in 10 binary logistic regression models, including the null model (Table 3). All models, except those fitted on the single variables x and P_7 , displayed significant β_h coefficients and likelihood ratio test ($p < 0.05$). A $\beta_h < 0$ was displayed by the model fitted on elevation el , indicating a negative correlation between altitude and the probability of infection. Conversely, for all the other tested variables, the logistic equations showed positive β_h coefficients, thereby indicating that an increasing probability of infection by *H. fraxineus* is expected with increasing values of the predictors. The AIC values ranged from 110.5 for the model that included both P_4 and P_7 to 124.2 for the model based uniquely on P_7 , corresponding to a maximum AICw of 68.2% and a minimum of 0.1%, respectively. The null model scored values of AIC = 123.2 and AICw = 0.1%. The AUC values ranged from a minimum of 0.50 (0.28–0.72 $CI_{95\%}$) for the null model to 0.75 (0.64–0.87 $CI_{95\%}$) for the model that included both P_4 and P_7 . Excluding the null model and that based on P_7 , all the others showed AUC $CI_{95\%}$ with bounds higher than the threshold of 0.5. Based on the criteria considering the highest AICw and AUC values, the best performing binary logistic regression model was based on P_4 and P_7 (Figure 2). The corresponding equation modelled a probability of infection by *H. fraxineus* close to 0% for ash trees growing in sites whose P_4 and P_7 were approximately around 10 and 40 mm, respectively, which jumped up to 80% when the above values increased to 60 and 80 mm (Figure 2). Instead, all other models based on binary logistic regressions scored worse than the model based on P_4 and P_7 , as shown in detail in Table 3.

The association between the probability of infection by *H. fraxineus* and the aspect (*as*) of the study site was not significant based on the results of the Mardia–Watson–Wheeler test ($p = 0.967$) and of the Rao’s homogeneity test ($p = 0.807$).

All variables of phytopathological, dendrometric, environmental or climatic interest obtained from this study are available in Table S3.

Table 3. Binary logistic regressions modelling the probability of infection by *Hymenoscyphus fraxineus*. For each input variable (see main text for acronyms definition), the associated β_h coefficient is reported along with its Wald test p -value (p), except for the null model for which no input variables are included. Asterisks next to the β_h mark significant values ($p < 0.05$). The models’ intercept β_0 and corresponding p -value are reported as well. The outcomes of the likelihood ratio test are indicated as a p -value in the column LRT, with the Akaike Information Criterion and weight (in %) being shown under the heading AIC and AICw, respectively. The area under the relative operating characteristic curve (AUC) and its cross-validated 95% confidence interval are included. The last column reports the ordinal score ranking the overall model performance from 1 (best performance) to 10 (worst performance).

Input Variable	$\beta_h(P)$	$\beta_0(P)$	LRT	AIC	AIC _w	AUC (CI _{95%})	Score
P_4, P_7	$\beta_{P_4}^* = 7.516 \cdot 10^{-2}$ ($P = 3.12 \cdot 10^{-4}$) $\beta_{P_7}^* = 5.315 \cdot 10^{-2}$ ($P = 1.48 \cdot 10^{-2}$)	$\beta_0 = -7.478$ ($P = 1.07 \cdot 10^{-4}$)	$P = 2.37 \cdot 10^{-4}$	110.46	68.2%	0.75 (0.64–0.87)	1
x, y	$\beta_x^* = 3.355 \cdot 10^{-5}$ ($P = 1.04 \cdot 10^{-2}$) $\beta_y^* = 1.307 \cdot 10^{-4}$ ($P = 3.53 \cdot 10^{-3}$)	$\beta_0 = -6.759 \cdot 10^2$ ($P = 3.17 \cdot 10^{-3}$)	$P = 1.65 \cdot 10^{-3}$	114.35	9.8%	0.71 (0.59–0.84)	2
P_{sp}	$\beta_{P_{sp}}^* = 2.762 \cdot 10^{-2}$ ($P = 3.41 \cdot 10^{-3}$)	$\beta_0 = -5.301$ ($P = 5.38 \cdot 10^{-4}$)	$P = 1.23 \cdot 10^{-3}$	114.71	8.2%	0.71 (0.59–0.82)	3
P_4	$\beta_{P_4}^* = 5.988 \cdot 10^{-2}$ ($P = 5.72 \cdot 10^{-3}$)	$\beta_0 = -3.648$ ($P = 4.44 \cdot 10^{-4}$)	$P = 1.44 \cdot 10^{-3}$	115	7.1%	0.70 (0.59–0.81)	4
T_{max12}	$\beta_{T_{max12}}^* = 2.815 \cdot 10^{-1}$ ($P = 4.41 \cdot 10^{-3}$)	$\beta_0 = -2.210$ ($P = 2.13 \cdot 10^{-5}$)	$P = 2.27 \cdot 10^{-3}$	115.84	4.6%	0.69 (0.58–0.80)	5
y	$\beta_y^* = 9.546 \cdot 10^{-5}$ ($P = 1.73 \cdot 10^{-2}$)	$\beta_0 = -4.848 \cdot 10^2$ ($P = 1.71 \cdot 10^{-2}$)	$P = 1.39 \cdot 10^{-2}$	119.11	0.9%	0.64 (0.51–0.76)	6
el	$\beta_{el}^* = -2.794 \cdot 10^{-3}$ ($P = 1.92 \cdot 10^{-2}$)	$\beta_0 = 1.993$ ($P = 1.16 \cdot 10^{-1}$)	$P = 1.53 \cdot 10^{-2}$	119.28	0.8%	0.64 (0.51–0.76)	7
x	$\beta_x = 2.124 \cdot 10^{-5}$ ($P = 7.40 \cdot 10^{-2}$)	$\beta_0 = -8.754$ ($P = 4.49 \cdot 10^{-2}$)	$P = 7.33 \cdot 10^{-2}$	121.95	0.2%	0.64 (0.53–0.76)	8
P_7	$\beta_{P_7} = 1.539 \cdot 10^{-2}$ ($P = 3.36 \cdot 10^{-1}$)	$\beta_0 = -1.925$ ($P = 5.37 \cdot 10^{-2}$)	$P = 3.35 \cdot 10^{-1}$	124.23	0.1%	0.57 (0.44–0.69)	9
- (null model)	-	$\beta_0 = 9.985 \cdot 10^{-1}$ ($P = 6.28 \cdot 10^{-6}$)	-	123.16	0.1%	0.50 (0.28–0.72)	10

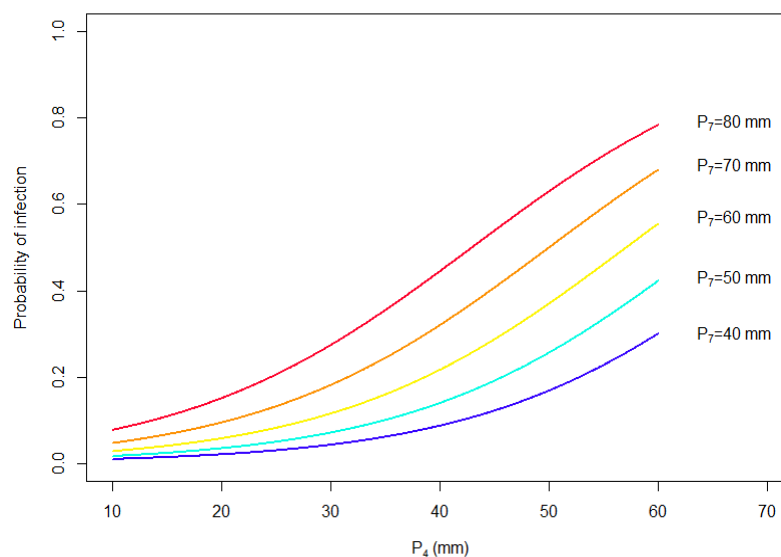


Figure 2. Binary logistic regression modelling the probability of infection by *Hymenoscyphus fraxineus* as a function of the cumulated precipitation of the months of April (P_4) and July (P_7) (in mm). The probability is indicated on the y-axis and it is expressed as a number in the interval [0–1]. The level of precipitation P_4 is reported on the x-axis (in mm) as a continuous variable, while P_7 is categorized in five classes from 40 to 80 mm, corresponding to distinct curves.

3.3. Spatial Gradients of the Impact of *Hymenoscyphus fraxineus*

The application of the DirGrad algorithm showed a decreasing spatial gradient of the incidence of *H. fraxineus* from north to south (N→S), NE→SW ($R = \mp 0.43$, the prevailing direction), E→W, and SE→NW (Figure 3). Although with different magnitudes of R and prevailing directions, the same decreasing spatial gradients with directions NE→SW, E→W were detected for the crown transparency (*crtr*), percentage of necrotic leaves (*pnl*), and number of lesions observed at the stem base of the ash trees (*nl*). Depending on the variable considered, other directions identified by the algorithm included N→S (*nl*, *pnl*), SE→NW (*crtr*, *nl*), and S→N (*crtr*) (Figure 3).

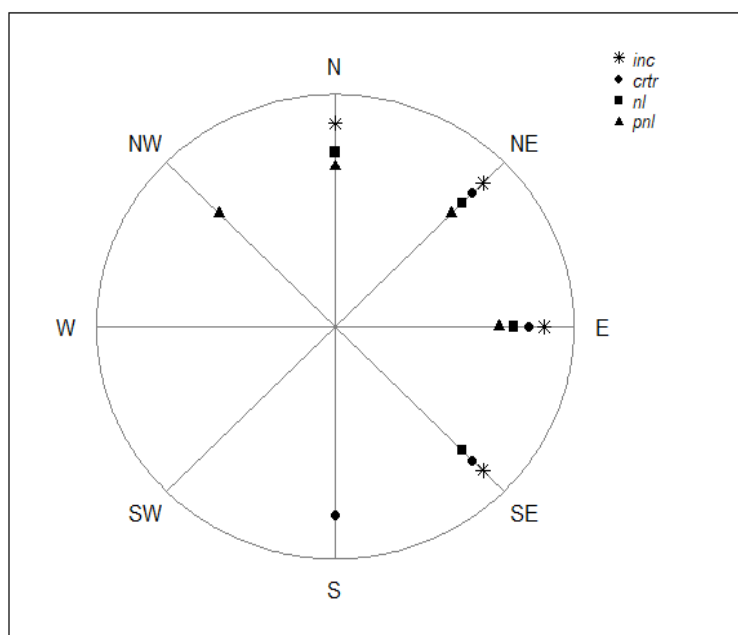


Figure 3. Windrose directional graph of the descending spatial gradients resulting from the incidence and impact of *Hymenoscyphus fraxineus* on ash trees in the inner-alpine valleys of northwestern Italy.

Directions marked with dots display values of the associated variable higher than those detected in the opposite direction. Variable acronyms are defined as follows: incidence of *H. fraxineus* (*inc*), ash crown transparency (*crtr*), number of lesions observed at the stem base (*nl*), and percentage of leaves displaying necrotic areas on the lamina (*pnl*).

A decreasing spatial gradient was detected for the monthly precipitation of April (P_4) with directions NE→SW, E→W, SE→NW, and S→N, with SE→NW as the prevailing direction ($R = \mp 0.53$). Instead, the rainfall of July (P_7) displayed a different trend with directions N→S, NW→SE, W→E, and SW→NE, with N→S ($R = \mp 0.62$) as the prevailing direction in this case.

The results obtained from the DirGrad algorithm are reported in Table S4.

3.4. Presence and Distribution of *Hymenoschyphus albidus*

The molecular analyses based on the species-specific qPCR assays did not detect the presence of *H. albidus* DNA either in the foliar or in wood samples collected from the monitored ash trees.

4. Discussion

Despite the widespread occurrence of *Hymenoschyphus fraxineus* in Europe, there are still some areas where its presence, abundance, and impact are still largely unknown. The inner-alpine valleys of northwestern Italy are one such area, and our study reports for the first time *H. fraxineus* to be present there in over 65% of the investigated forest stand and with an overall incidence of 27%. Although the above values might look mild, especially if compared with reports from other European regions [14,16,17], peaks of incidence of 80% were observed locally. In addition, the severity of the ash dieback symptoms observed was remarkable, attaining averages as high as 47% for the crown transparency, 46% for the leaves displaying necrotic areas on the lamina, and 1.7 for the average number of lesions observed at the stem base. Nonetheless, no mortality was detected among the sampled ash trees, and in one third of the sampling sites the pathogen was not present. Overall, our data may suggest that the local populations of *F. excelsior*, or at least some genotypes, could be partially tolerant to the disease; the genotypes of the pathogen present in the area display mild virulence; the ecological and/or environmental conditions are not completely favorable to the disease; or the invasion of *H. fraxineus* in the region is recent. It should be noted that the above hypotheses are not mutually exclusive, and, even though our experimental design cannot confirm or rule out some of them, for others we gathered clues shedding light on the reasons underlying the observed distribution and impact of ash dieback.

Previous studies focused on the population genetics of ash and on the host–pathogen interaction [12,74,75] reported that some genotypes display some tolerance against *H. fraxineus*, and that such tolerance is particularly pronounced in 1%–5% of the ash trees. This evidence seems to be confirmed by our empirical observations, showing that neighboring trees growing in the same study sites and under the same environmental conditions could be either infected or uninfected and could be characterized by different levels of the severity of symptoms. For instance, none of the sites surveyed for the presence of *H. fraxineus* showed an incidence of the pathogen attaining 100% or, as previously mentioned, appreciable mortality rates. However, our monitoring targeted a large majority of adult ashes, which are probably less likely to die than younger ones [76]. Unfortunately, no information about the population genetics of ash trees in that region is available; hence, the genetic resistance of the host to ash dieback cannot be either confirmed or excluded based on this study. In addition, to assess whether, and to what extent, a genetic host resistance may have exerted a role in the infection and impact patterns of *H. fraxineus*, comparative inoculation experiments are needed.

The presence of *H. fraxineus* explains most of the symptom severity observed during the monitoring of ash dieback in the study area, especially in relation to the crown trans-

parency, percentage of necrotic leaves, and number of lesions at the stem base. Nonetheless, a baseline level of the above symptoms was also detected in uninfected trees, probably due to other biotic or abiotic stressors. For instance, it was recently documented that other fungal species belonging to the family of Botryosphaeriaceae, such as *Diplodia fraxini* (Fr.) Fr. and *D. subglobosa* A.J.L. Phillips, Deidda & Linald., may determine disease symptoms similar to dieback on *F. excelsior* [77,78]. Indeed, many species of that family are well known as endophytes or the latent pathogens of woody plants, whose pathogenic switch and aggressiveness on the host may follow the onset of other conditions of general stress due to climatic factors [79]. However, since our study targeted ash dieback associated with *H. fraxineus*, no other fungal species were screened through isolation or molecular diagnostics, with the only exception being *H. albidus*.

Recently, studies focused on the impact of climate change in the Alpine district of northwestern Italy have reported an increased aridity and evapotranspiration trend [80], which has been previously associated with the decline of other forest tree species in the area, such as *Pinus sylvestris* L. Considering the ecology of ash and, in particular, its need for an adequate water supply [81], aridity may have played a role as stressor contributing to the onset of the baseline symptoms observed. Nonetheless, since infected ash trees displayed a level of symptom severity consistently and significantly higher than those uninfected, the role of *H. fraxineus* as the causal agent of the decline of ash in the area seems of primary importance.

Prioritizing the conservation efforts in areas where *H. fraxineus* is more unlikely to rise may be a key strategy to perpetuate the presence and to increase the abundance of ash trees. For this reason, quantitative tools unravelling the relation between the presence of the pathogen and the environmental conditions of the forest stands are needed. Overall, our modelling approach allowed us to test and quantify the effects of a wide set of environmental variables on the probability of infection by *H. fraxineus* on ash. A total of two dendrometric, three geomorphologic, three topographic, and eighty climatic variables were assessed as potential predictors of the risk of infection. Despite this high number of predictors, our modelling is statistically robust and reliable, because it is based on a mixed approach combining unbiased recursive binary partitioning trees and conditional inference with binary logistic regression, while the circular variables were handled with specific standalone techniques [32,47,52,55–58,64,67].

The lack of correlation between the probability of infection by *H. fraxineus* and the dendrometric variables (the diameter at breast height and tree height) suggests that the pathogen can affect ash trees of different ages and positions (i.e., dominant or dominated trees). Other studies have reported that the pathogen can infect its host regardless of the tree age in forest stands as well as in plantations or nurseries [14,16,17], although some reports indicate that larger trees could be less affected than smaller ones [35,82].

Among the geomorphological variables, elevation proved to be inversely correlated with the probability of infection by *H. fraxineus*, with high risk levels in stands at lower altitudes. Remarkably, our models detected ~900 m a.s.l. as the critical threshold of the elevation to discriminate between a high and low risk of infection, which is a value rather close to the limit of 1000 m a.s.l. estimated by Giongo et al. (2017) [26]. Indeed, in agreement with our results, the latter study showed that in the Eastern Alps the impact of ash dieback was substantially higher in those stands whose altitude was lower than the critical threshold. Since elevation is correlated with other environmental variables, and especially with climate (e.g., temperatures and precipitation) [83], it could be argued that a more thorough understanding of the risk of infection could be achieved by testing climatic variables as potential predictors, which was precisely the goal of our modelling approach. Nonetheless, the elevation of the forest stand is a piece of information that is easy to retrieve or measure, while the climatic characterization of sites may be challenging or impractical to conduct.

Our models showed that the most relevant predictors of the probability of infection by *H. fraxineus* were the precipitation levels of April and July. Higher precipitation levels

were positively correlated to a rising likelihood of infection, with a probability reaching a peak of 80% when such precipitation was maximal. These results are consistent with the information reported in other studies [26,28] and in reviews of previous lines of evidence from the available literature [8,36,37,84]. Indeed, more abundant precipitation, especially during the summer, should boost the infection by *H. fraxineus*. For instance, in France, ash trees growing under moist conditions or in stands located in more humid topographical positions were associated with a higher severity of ash dieback, especially in relation to the abundance of basal lesions [35]. The role of precipitation may be related to the sporulation pattern of the pathogen, potentially influencing not only the production and release of infectious ascospores but also of conidia, whose role in the biological cycle of the pathogen is pivotal and facilitates gene flow between sympatric strains [85]. The amount of *H. fraxineus* spores released per day has been positively correlated to the leaf surface moisture [86] that is more likely to be maintained in the rainiest locations, rather than in arid sites. Abundant rainfalls might also promote high humidity in the litter, boosting the ability of *H. fraxineus* mycelium to survive and further colonize ash tissues, especially those which serve as a substrate for the production of apothecia. Remarkably, *H. fraxineus* can form apothecia on leaf rachises and petioles of ash not only during the year after leaf fall, but also for up to five growing seasons after the leaves have been dropped [87].

The role of temperature on the risk of infection by *H. fraxineus* is more controversial. While in the Eastern Alps it was reported that high temperatures combined with high precipitation and humidity levels occurring during the growing season could be favorable to *H. fraxineus* [26], at the European scale the risk of the natural spread of the pathogen has been associated with lower air temperatures [37]. Another study has clearly shown that high summer temperatures hinder the sporulation potential of *H. fraxineus* [27]. Our models showed that warming maximum temperatures in December might boost the risk of infection by *H. fraxineus*. Nevertheless, there is no evidence of a relationship between winter temperatures and the biology of *H. fraxineus*. In the alpine context, this might be a peculiarity or, more likely, an effect of variable collinearity (e.g., with elevation or precipitation), which may arise when dealing with a large amount of complex ecological data.

The modelling of the spatial gradients showed that the incidence of *H. fraxineus* and the levels of the symptom severity followed a sizeable and consistent spatial pattern, with the highest values located in the NE and E sectors, followed by the N and SE ones. Conversely, the opposite sectors displayed the lowest values. The coefficients provided by the DirGrad algorithm [67] suggest that the provenance of the front of invasion of *H. fraxineus* was from the bordering Italian region of Piedmont (i.e., from E and SE) and from Switzerland (i.e., from NE and N). The tree models confirmed this result by identifying the NE sector as that displaying the highest probability of infection by *H. fraxineus*. It should be noted that the front of invasion of *H. fraxineus* in Italy likely moved from E to W, namely from Friuli (where the pathogen was first reported in 2009) [29] to Piedmont (where the first report was in 2016) [30]. Conversely, in Switzerland the front has been documented to have moved from the northern areas (in 2008) to the southern cantons bordering with the Aosta Valley (in 2013) (see map in [88]). Hence, it can be hypothesized that the front of invasion in the Aosta Valley derives from a combination of the fronts from Piedmont and Switzerland. It should be noted that the windborne infectious ascospores and the related spread of *H. fraxineus* seem not to have been hindered by topographic barriers [26], and the prevailing wind direction in the Aosta Valley is from E to W [89]. Hence, although *H. fraxineus* has been present in France since 2008 [35], its introduction from that country seems rather unlikely. While no historical information is available to confirm the spatial progression of the front of invasion in the western Italian Alps, the spatial gradient is unlikely to depend on environmental variables. Indeed, the most relevant predictors of the risk of infection by *H. fraxineus*, namely, the combined rainfalls of April and July, do not consistently follow the same spatial pattern of the incidence of the pathogen and of the severity of the symptoms. The presence of a spatial gradient of the incidence of *H. fraxineus* suggests that the invasion process is still ongoing in the Aosta Valley. As a result, the introduction of the pathogen is

relatively recent (probably after 2013–2016 based on the data from Gonthier et al. (2016) and Schoebel et al. (2018) [30,88]).

The attempt to test whether a replacement of *H. albidus* with *H. fraxineus* has occurred by following the approach reported in Garbelotto et al. (2022) [18] was not conclusive, since *H. albidus* was never detected in the study area.

5. Conclusions

In conclusion, our study reports for the first time the presence, spatial distribution, and incidence of *H. fraxineus* in the inner-alpine valleys of northwestern Italy, along with the severity of ash dieback. The modelling approach used in this work shows that rainfalls are the most relevant and significant predictors to quantify the probability of infection by *H. fraxineus*, which is boosted by increased precipitation in April and July. Other relevant environmental variables included the elevation, maximal temperatures, latitude, and longitude. The different model equations setting out the above probability are provided. Finally, the front of invasion likely moved from Italy and Switzerland, rather than from France, following a main direction from east to west, while the replacement of *H. albidus* is uncertain.

Supplementary Materials: The following supporting information can be downloaded at: <https://www.mdpi.com/article/10.3390/f15040732/s1>, Table S1: the weather stations used for the climatic characterization of the study sites; Table S2: the results from the fitting of unbiased recursive binary partitioning tree models based on conditional inference; Table S3: the raw data used for the modelling; Table S4: the decreasing spatial gradients of the incidence and impact of *Hymenoscyphus fraxineus* and of the monthly precipitation of April and July.

Author Contributions: Conceptualization, G.L. and P.G.; methodology, G.L. and S.P.; software, G.L.; validation, G.L., S.O. and S.P.; formal analysis, G.L., S.P. and P.G.; investigation, G.L., S.O., S.P. and M.G.; resources, P.G.; data curation, G.L. and S.O.; writing—original draft preparation, G.L.; writing—review and editing, P.G.; visualization, G.L., S.O., S.P. and M.G.; supervision, P.G.; project administration, P.G.; and funding acquisition, P.G. All authors have read and agreed to the published version of the manuscript.

Funding: This research was funded by the European Commission through the INTERREG V-A Italy–Switzerland Programme 2014–2020, Project MONGEFITOFOR id 540693 (linee guida per il MONitoraggio e la Gestione delle Emergenze FITOsanitarie nelle FOReste delle Alpi centro-occidentali). This research was also partially funded by a grant from the University of Torino (ex 60%).

Data Availability Statement: All data relevant to this study are provided as Supplementary Material.

Acknowledgments: The authors wish to thank the Forestry Corps of the Autonomous Region of Valle d’Aosta (Struttura Corpo Forestale della Valle d’Aosta), in particular Commander Luca Dovigo and Ivan Rollet, for the technical and logistical support; and the official climatic data provider of the Autonomous Region of Valle d’Aosta (Centro funzionale e pianificazione), in particular Sara Maria Ratto, for the provision of the time series of the climatic variables. The authors also wish to thank Simone Prospero of the Swiss Federal Research Institute WSL, Birmensdorf, Switzerland, for the useful advice on ash dieback monitoring and samplings and Daniel Rigling (WSL) for providing the reference isolates.

Conflicts of Interest: The authors declare no conflicts of interest. The funders had no role in the design of this study; in the collection, analyses, or interpretation of the data; in the writing of the manuscript; or in the decision to publish the results.

References

1. Bendel, M.; Kienast, F.; Bugmann, H.; Rigling, D. Incidence and distribution of *Heterobasidion* and *Armillaria* and their influence on canopy gap formation in unmanaged mountain pine forests in the Swiss Alps. *Eur. J. Plant Pathol.* **2006**, *116*, 85–93. [[CrossRef](#)]
2. Ferracini, C.; Saitta, V.; Rondoni, G.; Rollet, I. Variables affecting the pine processionary moth flight: A survey in the north-western Italian Alps. *Forests* **2022**, *14*, 31. [[CrossRef](#)]
3. Smidt, S. Assessment of air pollution stress on forest ecosystems by the example of the northern Tyrolean Limestone Alps. *J. Plant Physiol.* **1996**, *148*, 287–295. [[CrossRef](#)]

4. Csilléry, K.; Kunstler, G.; Courbaud, B.; Allard, D.; Lassègues, P.; Haslinger, K.; Gardiner, B. Coupled effects of wind-storms and drought on tree mortality across 115 forest stands from the western Alps and the Jura mountains. *Glob. Change Biol.* **2017**, *23*, 5092–5107. [[CrossRef](#)]
5. Albrich, K.; Rammer, W.; Seidl, R. Climate change causes critical transitions and irreversible alterations of mountain forests. *Glob. Change Biol.* **2020**, *26*, 4013–4027. [[CrossRef](#)] [[PubMed](#)]
6. Camerano, P.; Terzuolo, P.G.; Varese, P. *I Tipi Forestali della Valle d'Aosta*; Compagnia delle Foreste: Arezzo, Italy, 2007.
7. Ferretti, F.; Alberti, G.; Badalamenti, E.; Campagnaro, T.; Corona, P.; Garbarino, M.; La Mantia, T.; Malandra, F.; Maresi, G.; Morresi, D.; et al. *Boschi di Neoformazione in Italia: Approfondimenti Conoscitivi e Orientamenti Gestionali*; Consiglio per la Ricerca in Agricoltura e l'Analisi dell'Economia Agraria: Roma, Italy, 2019.
8. Pautasso, M.; Aas, G.; Queloz, V.; Holdenrieder, O. European ash (*Fraxinus excelsior*) dieback—A conservation biology challenge. *Biol. Conserv.* **2013**, *158*, 37–49. [[CrossRef](#)]
9. Kowalski, T. *Chalara fraxinea* sp. nov. associated with dieback of ash (*Fraxinus excelsior*) in Poland. *Forest Pathol.* **2006**, *36*, 264–270. [[CrossRef](#)]
10. Queloz, V.; Grünig, C.R.; Berndt, R.; Kowalski, T.; Sieber, T.N.; Holdenrieder, O. Cryptic speciation in *Hymenoscyphus albidus*. *Forest Pathol.* **2011**, *41*, 133–142. [[CrossRef](#)]
11. Kowalski, T.; Łukomska, A. Studies on *Fraxinus excelsior* L. dieback in Włoszczowa Forest Unit stands. *Acta Agrobot.* **2005**, *59*, 429–440.
12. McKinney, L.V.; Nielsen, L.R.; Collinge, D.B.; Thomsen, I.M.; Hansen, J.K.; Kjær, E.D. The ash dieback crisis: Genetic variation in resistance can prove a long-term solution. *Plant Pathol.* **2014**, *63*, 485–499. [[CrossRef](#)]
13. Hultberg, T.; Sandström, J.; Felton, A.; Öhman, K.; Rönnerberg, J.; Witzell, J.; Cleary, M. Ash dieback risks an extinction cascade. *Biol. Conserv.* **2020**, *244*, 108516. [[CrossRef](#)]
14. Hill, L.; Jones, G.; Atkinson, N.; Hector, A.; Hemery, G.; Brown, N. The £15 billion cost of ash dieback in Britain. *Curr. Biol.* **2019**, *29*, R315–R316. [[CrossRef](#)] [[PubMed](#)]
15. Petucco, C.; Lobianco, A.; Caurila, S. Economic evaluation of an invasive forest pathogen at a large scale: The case of ash dieback in France. *Environ. Model. Assess.* **2020**, *25*, 1–21. [[CrossRef](#)]
16. Timmermann, V.; Børja, I.; Hietala, A.M.; Kirisits, T.; Solheim, H. Ash dieback: Pathogen spread and diurnal patterns of ascospore dispersal, with special emphasis on Norway. *EPPO Bull.* **2011**, *41*, 14–20. [[CrossRef](#)]
17. Coker, T.L.R.; Rozsypálek, J.; Edwards, A.; Harwood, T.P.; Butfofy, L.; Buggs, R.J.A. Estimating mortality rates of European ash (*Fraxinus excelsior*) under the ash dieback (*Hymenoscyphus fraxineus*) epidemic. *Plants People Planet* **2019**, *1*, 48–58. [[CrossRef](#)]
18. Garbelotto, M.; Lione, G.; Martiniuc, A.V.; Gonthier, P. The alien invasive forest pathogen *Heterobasidion irregulare* is replacing the native *Heterobasidion annosum*. *Biol. Invasions* **2022**, *24*, 2335–2349. [[CrossRef](#)]
19. Kozanitas, M.; Osmundson, T.W.; Linzer, R.; Garbelotto, M. Interspecific interactions between the Sudden Oak Death pathogen *Phytophthora ramorum* and two sympatric *Phytophthora* species in varying ecological conditions. *Fungal Ecol.* **2017**, *28*, 86–96. [[CrossRef](#)]
20. Brasier, C.M.; Buck, K.W. Rapid evolutionary changes in a globally invading fungal pathogen (Dutch elm disease). *Biol. Invasions* **2001**, *3*, 223–233. [[CrossRef](#)]
21. McKinney, L.V.; Thomsen, I.; Kjær, E.; Bengtsson, S.; Nielsen, L. Rapid invasion by an aggressive pathogenic fungus (*Hymenoscyphus pseudoalbidus*) replaces a native decomposer (*Hymenoscyphus albidus*): A case of local cryptic extinction? *Fungal Ecol.* **2012**, *5*, 663–669. [[CrossRef](#)]
22. Hietala, A.M.; Agan, A.; Nagy, N.E.; Børja, I.; Timmermann, V.; Drenkhan, R.; Solheim, H. The native *Hymenoscyphus albidus* and the invasive *Hymenoscyphus fraxineus* are similar in their necrotrophic growth phase in ash leaves. *Front. Microbiol.* **2022**, *13*, 892051. [[CrossRef](#)]
23. Gross, A.; Zaffarano, P.L.; Duo, A.; Grünig, C.R. Reproductive mode and life cycle of the ash dieback pathogen *Hymenoscyphus pseudoalbidus*. *Fungal Genet. Biol.* **2012**, *49*, 977–986. [[CrossRef](#)] [[PubMed](#)]
24. Gross, A.; Holdenrieder, O.; Pautasso, M.; Queloz, V.; Sieber, T.N. *Hymenoscyphus pseudoalbidus*, the causal agent of European ash dieback. *Mol. Plant Pathol.* **2014**, *15*, 5–21. [[CrossRef](#)] [[PubMed](#)]
25. Grosdidier, M.; Ioos, R.; Husson, C.; Cael, O.; Scordia, T.; Marçais, B. Tracking the invasion: Dispersal of *Hymenoscyphus fraxineus* airborne inoculum at different scales. *FEMS Microbiol. Ecol.* **2018**, *94*, fiy049. [[CrossRef](#)] [[PubMed](#)]
26. Giongo, S.; Longa, C.M.O.; Dal Maso, E.; Montecchio, L.; Maresi, G. Evaluating the impact of *Hymenoscyphus fraxineus* in Trentino (Alps, Northern Italy): First investigations. *iForest* **2017**, *10*, 871–878. [[CrossRef](#)]
27. Grosdidier, M.; Ioos, R.; Marçais, B. Do higher summer temperatures restrict the dissemination of *Hymenoscyphus fraxineus* in France? *Forest Pathol.* **2018**, *48*, e12426. [[CrossRef](#)]
28. Migliorini, D.; Luchi, N.; Nigrone, E.; Pecori, F.; Pepori, A.L.; Santini, A. Expansion of ash dieback towards the scattered *Fraxinus excelsior* range of the Italian peninsula. *Biol. Invasions* **2022**, *24*, 1359–1373. [[CrossRef](#)]
29. Ogris, N.; Hauptman, T.; Jurc, D.; Floreanci, V.; Marsich, F.; Montecchio, L. First report of *Chalara fraxinea* on common ash in Italy. *Plant Dis.* **2010**, *94*, 133. [[CrossRef](#)] [[PubMed](#)]

30. Gonthier, P.; Giordano, L.; Sillo, F.; Martinis, R.; Pasi, V.; Rettori, A.A.; Tantardini, A. Sos cedri e frassini—Passaggio a Nord Ovest. *Acer* **2016**, *6*, 25–29.
31. Santini, A.; Ghelardini, L.; De Pace, C.; Desprez-Loustau, M.L.; Capretti, P.; Chandelier, A.; Cech, T.; Chira, D.; Diamandis, S.; Gaitniekis, T.; et al. Biogeographical patterns and determinants of invasion by forest pathogens in Europe. *New Phytol.* **2013**, *197*, 238–250. [[CrossRef](#)]
32. Lione, G.; Gonthier, P.; Garbelotto, M. Environmental factors driving the recovery of bay laurels from *Phytophthora ramorum* infections: An application of numerical ecology to citizen science. *Forests* **2017**, *8*, 293. [[CrossRef](#)]
33. Enderle, R.; Stenlid, J.; Vasaitis, R. An overview of ash (*Fraxinus* spp.) and the ash dieback disease in Europe. *CABI Rev.* **2019**, *14*, 1–12. [[CrossRef](#)]
34. Havrdová, L.; Zahradník, D.; Romportl, D.; Pešková, V.; Černý, K. Environmental and silvicultural characteristics influencing the extent of ash dieback in forest stands. *Baltic For.* **2017**, *23*, 168–182.
35. Marçais, B.; Husson, C.; Godart, L.; Cael, O. Influence of site and stand factors on *Hymenoscyphus fraxineus*-induced basal lesions. *Plant Pathol.* **2016**, *65*, 1452–1461. [[CrossRef](#)]
36. Grosdidier, M.; Scordia, T.; Ioos, R.; Marçais, B. Landscape epidemiology of ash dieback. *J. Ecol.* **2020**, *108*, 1789–1799. [[CrossRef](#)]
37. Dal Maso, E.; Montecchio, L. Risk of natural spread of *Hymenoscyphus fraxineus* with environmental niche modelling and ensemble forecasting technique. *Forest Res.* **2014**, *3*, 1000131. [[CrossRef](#)]
38. Havrdová, L.; Novotná, K.; Zahradník, D.; Buriánek, V.; Pešková, V.; Šrůtka, P.; Černý, K. Differences in susceptibility to ash dieback in Czech provenances of *Fraxinus excelsior*. *Forest Pathol.* **2016**, *46*, 281–288. [[CrossRef](#)]
39. Marciulyniene, D.; Davydenko, K.; Stenlid, J.; Cleary, M. Can pruning help maintain vitality of ash trees affected by ash dieback in urban landscapes? *Urban For. Urban Green.* **2017**, *27*, 69–75. [[CrossRef](#)]
40. Klesse, S.; Abegg, M.; Hopf, S.E.; Gossner, M.M.; Rigling, A.; Quelo, V. Spread and severity of ash dieback in Switzerland—tree characteristics and landscape features explain varying mortality probability. *Front. For. Glob. Chang.* **2021**, *4*, 645920. [[CrossRef](#)]
41. Cerutti, A.V.; Careggio, P.P.; De Leo, S.; Freydoz, M.C.; Ceragioli, L.; Prinetti, F. *Il Territorio e l'uomo in Valle d'Aosta—Parte I*; Edizioni AIIG.: Aosta, Italy, 2010.
42. Regione Autonoma Valle d'Aosta. Geoportale SCT—Sistema delle Conoscenze Territoriali—Assessorato Opere Pubbliche, Territorio e Ambiente—Dipartimento Programmazione, Risorse Idriche e Territorio—Pianificazione Territoriale—Ufficio Cartografico. 2013. Available online: <https://geoportale.regione.vda.it/> (accessed on 15 February 2024).
43. QGIS Development Team. QGIS Geographic Information System. Open Source Geospatial Foundation Project. QGIS 3.10 A Coruña. 2019. Available online: <https://qgis.org/en/site/> (accessed on 16 February 2024).
44. EPPO. PM 7/117 (1) *Hymenoscyphus pseudoalbidus*. *EPPO Bull.* **2013**, *43*, 449–461. [[CrossRef](#)]
45. Müller, E.; Stierlin, H.R. *Sanasilva Tree Crown Photos with Percentages of Foliage Loss*; Swiss Federal Institute for Forest, Snow, and Landscape Research: Birmensdorf, Switzerland, 1990.
46. Durrant, D.; Eichhorn, J.; Ferretti, M.; Roskams, P.; Szepesi, A. *Manual on Methods and Criteria for Harmonized Sampling, Assessment, Monitoring and Analysis of the Effects of Air Pollution on Forests, Part II, Visual Assessment of Crown Condition*; United Nations Economic Commission for Europe Convention on Long-Range Transboundary Air Pollution; United Nations: New York, NY, USA, 2006.
47. Lione, G.; Giordano, L.; Turina, M.; Gonthier, P. Hail-induced infections of the chestnut blight pathogen *Cryphonectria parasitica* depend on wound size and may lead to severe diebacks. *Phytopathology* **2020**, *110*, 1280–1293. [[CrossRef](#)]
48. Baral, H.-O.; Bemann, M. *Hymenoscyphus fraxineus* vs *Hymenoscyphus albidus*—A comparative light microscopic study on the causal agent of European ash dieback and related foliicolous, stroma-forming species. *Mycology* **2014**, *5*, 228–290. [[CrossRef](#)] [[PubMed](#)]
49. Chandelier, A.; André, F.; Laurent, F. Detection of *Chalara fraxinea* in common ash (*Fraxinus excelsior*) using real time PCR. *Forest Pathol.* **2010**, *40*, 87–95. [[CrossRef](#)]
50. Husson, C.; Scala, B.; Caël, O.; Frey, P.; Feau, N.; Ioos, R.; Marçais, B. *Chalara fraxinea* is an invasive pathogen in France. *Eur. J. Plant Pathol.* **2011**, *130*, 311–324. [[CrossRef](#)]
51. Dokmanic, I.; Parhizkar, R.; Ranieri, J.; Vetterli, M. Euclidean distance matrices: Essential theory, algorithms, and applications. *IEEE Signal Process. Mag.* **2015**, *32*, 12–30. [[CrossRef](#)]
52. Lione, G.; Brescia, F.; Giordano, L.; Gonthier, P. Effects of seasonality and climate on the propagule deposition patterns of the chestnut blight pathogen *Cryphonectria parasitica* in orchards of the Alpine district of north western Italy. *Agriculture* **2022**, *12*, 644. [[CrossRef](#)]
53. Mitchell, A. *The ESRI Guide to GIS Analysis, Volume 2: Spatial Measurements and Statistics*; ESRI Press: Redlands, CA, USA, 2009.
54. Crawley, M.J. *The R Book*, 2nd ed.; John Wiley and Sons Ltd.: West Sussex, UK, 2013.
55. Hosmer, D.W.; Lemeshow, S. *Applied Logistic Regression*; John Wiley and Sons Ltd.: Hoboken, NJ, USA, 1989.
56. Hothorn, T.; Hornik, K.; Zeileis, A. Unbiased recursive partitioning: A conditional inference framework. *J. Comput. Graph. Stat.* **2006**, *15*, 651–674. [[CrossRef](#)]
57. Zeileis, A.; Leisch, F.; Hornik, K.; Kleiber, C. strucchange: An R package for testing for structural change in linear regression models. *J. Stat. Softw.* **2002**, *7*, 1–38. [[CrossRef](#)]

58. Hothorn, T.; Zeileis, A. partykit: A modular toolkit for recursive partytioning in R. *J. Mach. Learn. Res.* **2015**, *16*, 3905–3909.
59. Gerber, H.U.; Leung, B.P.K.; Shiu, E.S.W. Indicator function and Hattendorff theorem. *N. Am. Actuar. J.* **2003**, *7*, 38–47. [[CrossRef](#)]
60. Wagenmakers, E.J.; Farrell, S. AIC model selection using Akaike weights. *Psychon. Bull. Rev.* **2004**, *11*, 192–196. [[CrossRef](#)]
61. Grueber, C.E.; Nakagawa, S.; Laws, R.J.; Jamieson, I.G. Multimodel inference in ecology and evolution: Challenges and solutions. *J. Evol. Biol.* **2011**, *24*, 699–711. [[CrossRef](#)] [[PubMed](#)]
62. Robin, X.; Turck, N.; Hainard, A.; Tiberti, N.; Lisacek, F.; Sanchez, J.C.; Müller, M. pROC: An open-source package for R and S+ to analyze and compare ROC curves. *BMC Bioinform.* **2011**, *12*, 77. [[CrossRef](#)] [[PubMed](#)]
63. LeDell, E.; Petersen, M.; van der Laan, M. Computationally efficient confidence intervals for cross-validated area under the ROC curve estimates. *Electron. J. Stat.* **2015**, *9*, 1583. [[CrossRef](#)] [[PubMed](#)]
64. Pewsey, A.; Neuhäuser, M.; Ruxton, G.D. *Circular Statistics in R*; Oxford University Press: Oxford, UK, 2013.
65. Mardia, K.V. A multi-sample uniform scores test on a circle and its parametric competitor. *J. R. Stat. Soc. Ser. B-Stat. Methodol.* **1972**, *34*, 102–113. [[CrossRef](#)]
66. Rao, J.S. Large sample tests for the homogeneity of angular data. *Sankhya Ser. B* **1967**, *28*, 172–174.
67. Lione, G.; Giraud, M.; Gonthier, P. Modelling the front dynamics of invasive plant pathogens through the analysis of spatial gradients. *J. Plant Pathol.* **2024**, submitted.
68. Zhang, B.; Bilder, C.; Biggerstaff, B.; Schaarschmidt, F.; Hitt, B.; binGroup: Evaluation and Experimental Design for Binomial Group Testing. R Package Version 2.2-1. 2018. Available online: <https://CRAN.R-project.org/package=binGroup> (accessed on 9 February 2024).
69. Efron, B.; Tibshirani, R.J. *An Introduction to the Bootstrap*; Chapman & Hall/CRC: New York, NY, USA, 1994.
70. Agostinelli, C.; Lund, U. R Package ‘Circular’: Circular Statistics (version 0.5-0). 2023. Available online: <https://CRAN.R-project.org/package=circular> (accessed on 9 February 2024).
71. Barton, K.; MuMIn: Multi-Model Inference. R Package Version 1.43.6. 2019. Available online: <https://cran.r-project.org/web/packages/MuMIn/index.html> (accessed on 9 February 2024).
72. Blaker, H. Confidence curves and improved exact confidence intervals for discrete distributions. *Can. J. Stat.-Rev. Can. Stat.* **2000**, *28*, 783–798. [[CrossRef](#)]
73. DiCiccio, T.J.; Efron, B. Bootstrap confidence intervals. *Stat. Sci.* **1996**, *11*, 189–228. [[CrossRef](#)]
74. McKinney, L.V.; Nielsen, L.R.; Hansen, J.K.; Kjær, E.D. Presence of natural genetic resistance in *Fraxinus excelsior* (Oleraceae) to *Chalara fraxinea* (Ascomycota): An emerging infectious disease. *Heredity* **2011**, *106*, 788–797. [[CrossRef](#)]
75. McKinney, L.V.; Thomsen, I.M.; Kjaer, E.D.; Nielsen, L.R. Genetic resistance to *Hymenoscyphus pseudoalbidus* limits fungal growth and symptom occurrence in *Fraxinus excelsior*. *Forest Pathol.* **2012**, *42*, 69–74. [[CrossRef](#)]
76. Timmermann, V.; Nagy, N.E.; Hietala, A.M.; Børja, I.; Solheim, H. Progression of ash dieback in Norway related to tree age, disease history and regional aspects. *Baltic For.* **2017**, *23*, 150–158.
77. Linaldeddu, B.T.; Bottecchia, F.; Bregant, C.; Maddau, L.; Montecchio, L. *Diplodia fraxini* and *Diplodia subglobosa*: The main species associated with cankers and dieback of *Fraxinus excelsior* in north-eastern Italy. *Forests* **2020**, *11*, 883. [[CrossRef](#)]
78. Linaldeddu, B.T.; Bregant, C.; Montecchio, L.; Brglez, A.; Piškur, B.; Ogris, N. First report of *Diplodia fraxini* and *Diplodia subglobosa* causing canker and dieback of *Fraxinus excelsior* in Slovenia. *Plant Dis.* **2022**, *106*, 26–29. [[CrossRef](#)] [[PubMed](#)]
79. Slippers, B.; Wingfield, M.J. Botryosphaeriaceae as endophytes and latent pathogens of woody plants: Diversity, ecology and impact. *Fungal Biol. Rev.* **2007**, *21*, 90–106. [[CrossRef](#)]
80. Orusa, T.; Borgogno Mondino, E. Exploring short-term climate change effects on rangelands and broad-leaved forests by free satellite data in Aosta Valley (Northwest Italy). *Climate* **2021**, *9*, 47. [[CrossRef](#)]
81. Kerr, G.; Cahalan, C. A review of site factors affecting the early growth of ash (*Fraxinus excelsior* L.). *For. Ecol. Manag.* **2004**, *188*, 225–234. [[CrossRef](#)]
82. Erfmeier, A.; Haldan, K.L.; Beckmann, L.M.; Behrens, M.; Rotert, J.; Schrautzer, J. Ash dieback and its impact in near-natural forest remnants—a plant community-based inventory. *Front. Plant Sci.* **2019**, *10*, 658. [[CrossRef](#)] [[PubMed](#)]
83. Beniston, M. Mountain weather and climate: A general overview and a focus on climatic change in the Alps. *Hydrobiologia* **2006**, *562*, 3–16. [[CrossRef](#)]
84. Ghelardini, L.; Migliorini, D.; Santini, A.; Pepori, A.L.; Maresi, G.; Vai, N.; Montuschi, C.; Carrari, E.; Feducci, M.; Capretti, P.; et al. From the Alps to the Apennines: Possible spread of ash dieback in Mediterranean areas. In *Dieback of European Ash (Fraxinus spp.)—Consequences and Guidelines for Sustainable Management*; Vasaitis, R., Enderle, R., Eds.; SLU Service/Repro: Uppsala, Sweden, 2017; pp. 140–149.
85. Fones, H.N.; Mardon, C.; Gurr, S.J. A role for the asexual spores in infection of *Fraxinus excelsior* by the ash-dieback fungus *Hymenoscyphus fraxineus*. *Sci. Rep.* **2016**, *6*, 34638. [[CrossRef](#)]
86. Burns, P.; Timmermann, V.; Yearsley, J.M. Meteorological factors associated with the timing and abundance of *Hymenoscyphus fraxineus* spore release. *Int. J. Biometeorol.* **2022**, *66*, 493–506. [[CrossRef](#)]
87. Kirisits, T. Ascocarp formation of *Hymenoscyphus fraxineus* on several-year-old pseudosclerotial leaf rachises of *Fraxinus excelsior*. *Forest Pathol.* **2015**, *45*, 254–257. [[CrossRef](#)]

-
88. Schoebel, C.N.; Prospero, S.; Gross, A.; Rigling, D. Detection of a conspecific mycovirus in two closely related native and introduced fungal hosts and evidence for interspecific virus transmission. *Viruses* **2018**, *10*, 628. [[CrossRef](#)] [[PubMed](#)]
 89. Centro Funzionale Regione Autonoma Valle d'Aosta 2024. Vento. Available online: <https://cf.regione.vda.it/vento.php> (accessed on 16 February 2024).

Disclaimer/Publisher's Note: The statements, opinions and data contained in all publications are solely those of the individual author(s) and contributor(s) and not of MDPI and/or the editor(s). MDPI and/or the editor(s) disclaim responsibility for any injury to people or property resulting from any ideas, methods, instructions or products referred to in the content.